BDNF-TrkB Pathway Mediates NMDA receptor NR2B Subunit Phosphorylation in the Supraoptic Nuclei Following Progressive Dehydration

Flávia Regina Carreño[1], **Joseph D Walch**[1,2], **Mayurika Dutta**[1], **Thekkethil P. Nedungadi**[1], and **J. Thomas Cunningham**[1]

[1]Department of Integrative Physiology, and Cardiovascular Research Institute, University of North Texas Health Science Center at Fort Worth, 3500 Camp Bowie Blvd, Fort Worth, TX 76107

[2]Department of Pharmacology and Neuroscience, University of Texas Health Science Center at San Antonio, 7703 Floyd Curl Drive, San Antonio, TX 78229

Abstract

We studied the effects of water deprivation on the phosphorylation of TrkB and NMDA receptor subunits in the supraoptic nucleus (SON) of the rat. Laser capture microdissection and qRT-PCR was used to demonstrate BDNF and TrkB gene expression in vasopressin SON neurones. Immunohistochemistry confirmed BDNF staining in vasopressin neurones, while staining for phosphorylated TrkB was increased following water deprivation. Western Blot analysis of brain punches containing the SON revealed that tyrosine phosphorylation of TrkB ($pTrkBY^{515}$), serine phosphorylation of NR1 ($pNR1S^{866}$ or pNR1) and tyrosine phosphorylation of NR2B subunits ($pNR2BY^{1472}$ or pNR2B) were significantly increased in WD animals compared to control. Access to water for 2 h reduced $pTrkBY^{515}$ content to control levels without affecting pNR1 or pNR2B. Four hours of rehydration was needed to reduce pNR1 and pNR2B to control. To test whether increased phosphorylation of TrkB in this study is mediated by BDNF, a group of animals were instrumented with right SON cannula coupled to mini-osmotic pumps filled with vehicle or TrkB-Fc fusion protein which prevents BDNF binding to TrkB. In the left SON contralateral to the cannula, TrkB phosphorylation was significantly enhanced following WD. Separate analysis of the right SON, which received TrkB-Fc, showed that the TrkB receptor phosphorylation following WD was significantly attenuated. While increased $pNR1S^{866}$ following WD was not affected by local infusion of TrkB-Fc, $pNR2BY^{1472}$ was significantly reduced. Co-immunoprecipitation revealed an increased physical interaction between Fyn kinase and NR2B and TrkB in the SON following water deprivation. Thus, activation of TrkB in the SON following WD may affect cellular excitability through the phosphorylation of NR2B subunits.

Keywords

vasopressin; NMDA receptor; BDNF; Osmotic Pressure

INTRODUCTION

Brain-derived neurotrophic factor (BDNF), a member of the nerve growth factor family (1), can modify the synaptic efficacy of neural circuitry in the adult brain (2-5). BDNF can affect

Corresponding author: J. Thomas Cunningham, Department of Integrative Physiology, University of North Texas Health Science Center at Fort Worth, 3500 Camp Bowie Blvd, Fort Worth, TX 76107, Phone: 817-735-5096, Fax: 817-735-5084, Tom.Cunningham@unthsc.edu.

synaptic inhibition by decreasing the surface stability and expression of γ-aminobutyric acid type A (GABA$_A$) (6-8). In glutamatergic synapses, BDNF has been shown to regulate α-amino-3-hydroxy-5-methyl-4-isoxazolepropionic acid (AMPA) and N-methyl-D-aspartate (NMDA) receptor subunit phosphorylation, trafficking, and expression (9-11) through the activation of tyrosine kinase B (TrkB) receptors.

BDNF and TrkB are both expressed in magnocellular neurosecretory cells (MNCs) in the supraoptic nucleus (SON) of the adult rat (12-14). These cells synthesize and secrete either oxytocin (OT) or arginine vasopressin (AVP) in to systemic circulation from axon terminals located in the posterior pituitary (15-17). Plasma osmolality is one of the main factors controlling the circulating levels of AVP, although increased plasma osmolality increases the activity of both AVP and oxytocin neurones (17-20). In vitro studies have demonstrated that MNCs are intrinsically osmosensitive (18, 21). In addition to intrinsic osmosensitivity, GABA and glutamate synaptic inputs also contribute to the regulation of MNCs and neurohypophyseal hormone release in response to osmotic stimulation (18, 19).

Following osmotic stress, BDNF mRNA is increased in SON peaking in advance of increased AVP protein content in the SON and PVN (22). Moreover, BDNF is released into the extracellular space of the SON after acute osmotic stimulation suggesting a putative autocrine or paracrine action in these nuclei via activation of TrkB and downstream signaling cascades (23). The physiologic significance of this signaling pathway has yet to be determined.

In vitro, BDNF exposure decreases the inhibitory effects of GABA on parvocellular neuroendocrine neurones from the paraventricular nucleus (PVN) of the hypothalamus (7). This effect is mediated by a postsynaptic mechanism dependent on TrkB receptor activation. In the SON, acute bath applications of BDNF decrease postsynaptic GABAergic activity without affecting spontaneous excitatory postsynaptic currents (14). Thus, BDNF could play a role in the synaptic activation of PVN and SON neurones by decreasing the membrane expression of postsynaptic GABA$_A$ receptors and reduce the postsynaptic inhibitory effects of GABA.

In addition to affecting GABA receptors, BDNF has been shown to enhance glutamatergic synaptic transmission in several systems (5, 9-11, 24, 25). In vitro, BDNF has been shown to enhance NMDA receptor-mediated postsynaptic responses in several different neural cells types (9, 10) and produce phosphorylation of NR1 and NR2 subunits (9, 10).

Chronic osmotic stimulation causes reversible changes in glutamatergic metabotropic (26) and ionotropic NMDA receptors in the SON (27, 28). Although the role of BDNF-TrkB signaling is involved in activity-dependent neuronal plasticity (25, 29, 30), its effects upon NMDA receptors in SON neurones have not yet been determined.

In the present studies, 48 hours water deprivation was used as a progressive homeostatic challenge to physiologically stimulate the SON (31, 32). We tested the effects of water deprivation alone or followed by 2 or 4 hours access to water (rehydration) on TrkB phosphorylation in the SON. To determine whether these effects could be BDNF-mediated pre-administration of the TrkB-Fc fusion protein in SON were conducted to prevent binding between BDNF and the TrkB (33-36). In addition, we investigated the effects of dehydration and BDNF-TrkB signaling on NR1 and NR2B expression and phosphorylation.

MATERIALS AND METHODS

Animals

Experiments were conducted on adult male Sprague–Dawley rats that weighed 250–350 g (Charles Rivers). Rats were individually housed and maintained in a temperature-controlled environment on a 14:10 h light–dark cycle. Experimental protocols were approved by the IACUC in accordance with the guidelines of the Public Health Service, the American Physiological Society, and the Society for Neuroscience. All rats had *ad libitum* access to food throughout the experiments unless otherwise indicated. The control group was allowed *ad libitum* access to water and food while water deprived animals had no access to water for 48 h. Two other groups of animals were water deprived for 46 hours followed by 2 or 4 h access to water prior to sacrifice (rehydration studies). During water access, the food was not available.

Micropunch dissection

Each rat was anesthetized with inactin (100 mg/Kg i.p.) and decapitated. The brain was removed from the skull and placed in a commercially available brain matrix (Stoelting). The matrix was used to cut the brain into 1 mm coronal slabs with doubled edges razor blades. Punches containing the SON were then collected from the slabs using 1 ml syringes equipped with blunt 23 gauge needles. The samples were placed in microcentrifuge tubes and rapidly frozen (37). Punches were sonicated in 35μl of modified RIPA-buffer supplemented with protease and phosphatase inhibitors followed by 30 min incubation on ice. The total homogenates were centrifuged 14,000 rpm, 30 min at 4°C to clear the lysate.

SON cannulation and osmotic minipump implantation

Alzet osmotic pumps (model 2004; 0.25 μl/h) were filled with sterile 0.9% saline (vehicle) or recombinant human TrkB-Fc Chimera (TrkB-Fc; Lot BUX0409011, R&D Systems; Minneapolis, MN) at a concentration of 200ng/ μl in 0.9% saline. The dosage of TrkB-Fc was chosen according to previous *in vivo* studies (33-36). Pumps were then attached to a catheter coupled to a cannula (38). The entire apparatus was primed overnight in sterile saline at 37°C. Rats were initially anesthetized with brevital (10 mg/kg ip) and, then positioned in a stereotaxic apparatus (Kopf Instruments, Tujunga, CA). Anesthesia was maintained with isofluorane (2%) delivered by a nose cone attached to the stereotaxic frame (Kopf Instruments, Tujunga, CA). The cannula (Plastics One, Roanoke, VA) was stereotaxically positioned in the right SON (1.2 mm caudal and 1.4 mm lateral from bregma, 8.8 mm ventral) and chronically fixed in place using two jeweler's screws and dental acrylic. Stereotaxic coordinates were determined from the rat brain atlas of Paxinos and Watson (39). The rats were allowed to recover for 3-4 days after surgery before being used in water deprivation experiments. After terminal experiments, rats were anesthetized (inactin 100 mg/kg ip), and decapitated. Punches were collected as described above. Brain punches containing the right (cannulated) and left (uncannulated) SON were placed in separate microcentrifuge tubes and rapidly frozen for analysis.

Western Blot analysis

Protein concentration of each sample was determined by Bradford method (40). Next, 10-40 ug of the total lysate were loaded onto a 7.5% or 10% acrylamide SDS gel, separated by electrophoresis in Tris-glycine buffer with denaturing conditions and transferred to nitrocellulose membrane (BioRad) in Tris-glycine buffer (25mM Tris, 250mM Glycine, 0.1% SDS; pH 8.3) with 20% methanol. Membranes were blocked with 5% nonfat milk in Tris-buffered saline-Tween 20 (TBS-Tween; 25mM Tris base, 125 mM NaCl, 0.1% Tween 20) for 1 hour at room temperature. Next, they were incubated overnight at 4°C in 1%

nonfat milk in Tris-buffered saline with primary antibodies. The primary antibodies used in this study were: TrkB receptor (Neuromics; GT15080; lot#400622); NMDA receptor subunits: NR1 (Millipore; 07-362-MN; Lot# DAM1597365); NR2B (Millipore; 05-920; Lot# DAM1585439); Fyn kinase (Chemicon; MAB8900; Lot# LV1362411), GAPDH (Millipore; AB9132; Lot# LV1542016); phosphorylated TrkB (TrkBY[515]; Abcam; ab51187; Lot# 547336); phosphorylated NR1 subunit (pNR1S[866]; Millipore; 06-640-MN; Lot# DAM1597359); phosphorylated NR2B subunit (pNR2BY[1472]; PhosphoSolutions®; p1516-1472). Membranes were rinsed three times for ten minutes with TBS-Tween then incubated for 2 hours at room temperature with a horseradish peroxidase conjugated secondary antibody against the primary antibody host species (anti-goat, anti-rabbit and anti-chicken; all from SIGMA). The membranes were washed three times for ten minutes in TBS- Tween. Proteins were detected by enhanced chemiluminescence (ECL reagents, Amersham) and exposed to radiographic film (Hyperfilm ECL, Amersham). Digital images of the film were acquired (Adobe Photoshop CS3 Extend v10.0.1, Adobe Systems Incorporated, San Jose, CA) and densitometry of the bands was performed (Scion Image for Windows v4.0.3.2, Scion Corporation, Frederick, MD). Densitometric measurements of the immunoreactive bands were normalized using GAPDH.

Co-immunoprecipitation and immunoblotting

To study physical interaction between TrkB, Fyn and NR2B, co-immunoprecipitation assays were performed (41). Four punches containing the SONs from two rats of the same treatment group were pooled and lysed in ice-cold NP-40 buffer (1% Igepal, 0.15M NaCl, 0.01 M sodium phosphate, 0.002M EDTA pH 7.2) supplemented with protease and phosphatase inhibitors. The protein concentration of each homogenate was determined using the BCA method (Pierce). The total lysate (80-100 ug of protein) was incubated with anti-TrkB receptor antibody (4ug; (Neuromics; GT15080; lot#400622) at 4°C for 1h followed by precipitation with protein G-Sepharose beads (50ul) for 30 min at 4°C. The immunocomplexes were then washed and resuspended in sample buffer. Samples were boiled for 5 min, subjected to SDS-PAGE and immunoblotted using anti-Fyn (Chemicon; MAB8900; Lot# LV1362411) and anti-NR2B antibodies (Millipore; 05-920; Lot# DAM1585439). HRP conjugated anti-rabbit or anti-mouse secondary antibody (1:5000, Sigma) were used. Immunoreactive bands were detected by enhanced chemiluminescence (ECL reagents, Amersham) and exposed to radiographic film (Hyperfilm ECL, Amersham). Digital images of the film were acquired (Adobe Photoshop CS3 Extend v10.0.1, Adobe Systems Incorporated, San Jose, CA) and densitometry of the bands was performed (Scion Image for Windows v4.0.3.2, Scion Corporation, Frederick, MD).

Immunohistochemistry

Rats were anesthetized with inactin (100 mg/kg ip) and perfused transcardially with PBS followed by 4% paraformaldehyde. Each brain was prepared for immunohistochemistry as previously described (32). Separate sets of forebrain sections containing the SON were processed for either BDNF or pTrkBY[515] immunofluorescence. For BDNF staining, a chicken anti-BDNF polyclonal antibody (Abcam; 1:500) and a Cy3 conjugated donkey anti-chicken secondary antibody (Jackson ImmunoResearch; 1:250) were used. Separate sections were processed with a rabbit anti-pTrkBY[515] (Abcam; ab51187; 1:1000) and a biotinylated donkey anti-rabbit secondary antibody (Vector Labs, 1:250) and streptavidin Dylight 594 (Jackson ImmunoResearch; 1:250). Each set of sections also were processed for vasopressin immunofluorescence using a Guinea pig anti-(Arg8) Vasopressin primary antibody (Peninsula Laboratories, 1:10,000) and a Cy2 conjugated donkey anti-Guinea pig secondary antibody (1:250, Jackson ImmunoResearch, West Grove, PA). Sections were incubated in both primary antibodies for 2 days and 4°C. Sections were mounted on gelatin coated slides and cover slipped with hard set Vectashield (Vector Labs) mounting media.

Sections containing the supraoptic nucleus were analyzed for BDNF or pTrkBY[515] and AVP co-localization using a Qimaging camera attached to an IX50 Olympus converted to a DSU confocal microscope with an attached mercury lamp for fluorescence. Images were adjusted for uniform brightness and contrast, pseudocolored and merged using ImageJ software. Regions of interest were identified using the rat brain stereotaxic atlas of Paxinos and Watson (51).

Laser Capture Microdissection (LCM) of magnocellular vasopressinergic neurones

Rapid immunostaining of AVP neurones—Rats were anesthetized with inactin (100 mg/kg ip) and decapitated. Brains were frozen in cooled isopentane kept on dry ice, and 10μm thick serial frozen sections were cut through the hypothalamus at the level of the SON using a cryostat. The sections were mounted onto PEN membrane coated slides (Catalogue# LCM0522-Arcturus Bioscience). After the sections thawed for 30 s, they were fixed in ice-cold 100% methanol for 3 min followed by washing in cold DEPC-PBS for 3 times. Blocking was done in DEPC-PBS diluent for 5 min. This was followed by incubation in an Guinea pig anti-vasopressin antibody diluted 1:50 (Peninsula Laboratories) in DEPC-PBS diluent for 3 min and incubation in 1:50 donkey anti-guinea pig -Cy3 secondary antibody (Jackson ImmunoResearch) diluted in DEPC-PBS for 3 min.

Laser capture microdissection of the AVP neurones—An Arcturus Veritas Microdissection instrument, which utilizes the IR capture laser with a UV cutting laser, was used to laser capture AVP labeled neurones. Only neurones that exhibited a visible and complete staining of the cytoplasmic compartment was selected for harvesting. After dissociation of individual immunoreactive neurones from surrounding tissue, each cell was captured into an Arcturus Adhesive Cap. After capture, the cap was immediately transferred to a 0.5ml tube containing 30 μl of ArrayPure Nano-Scale Lysis Solution with 5.0 μg of proteinase K (prod. no. MPS04050; Epicentre Biotechnol Inc. Madison, WI, USA).

Single-neurone RNA extraction and amplification—Total RNA was isolated from each of 9-12 neurones collected per animal with ArrayPure Nano-Scale RNA Purification Kit reagents (Epicentre Biotechnol Inc.), in accordance with the manufacturer's instructions as previously described (42). The cells were incubated in Lysis Solution for 15 min at 65–70 °C, and protein was precipitated by addition of 18 μl of MPC Protein Precipitation, followed by vortexing and centrifugation at 10, 000 g for 7 min at 4 °C. Fifty microlitres of isopropanol was added to the supernatant, followed by centrifugation at 10, 000 g for 5 min at 4 °C. Contaminating DNA was removed from preparations: pellets were air-dried for 5 min, resuspended in 20 μl of DNase I solution containing 1 μl of RNase- Free DNase I and 40μl of 1X DNase buffer, and then incubated for 10 min. After addition of 20 μl each of 2X Nano-Scale Lysis Solution and MPC Protein Precipitation Reagent, the mixture was vortexed and centrifuged at 10, 000 g for 5 min at 4 °C. After the addition of 50 ul isopropanol, the supernatants were centrifuged at 10,000 g for 5 min at 4 °C to pellet purified RNA. Final rinsing was carried out with 70% ethanol. Resulting pellets were air-dried for 5 min, and resuspended in 5 μl of RNase-Free water supplemented with 1μl of ScriptGuard RNase inhibitor (Epicentre Biotechnol Inc.). All RNA samples were stored at − 80° C. The RNA content of each sample was evaluated using a Nanodrop Spectrophotometer. An 2 μl aliquot of cellular RNA sample was amplified with Target A m p 2-Round Aminoallyl-aRNA Amplification Kit materials (Epicentre Biotechnol Inc.), in accordance with the manufacturer's instructions to produce aminoallyl-aRNA, with partial substitution of the canonical UTP nucleotide by aminoallyl-UTP (42).

Single Cell qRT-PCR—Aminoallyl-aRNA (< 50 ng) from each laser-micro dissected neurone was reverse-transcribed to cDNA with Sensiscript RT Kit reagents (prod. no.

205213; Qiagen Inc., Valencia, CA, USA) as previously described (42). Each RT reaction mixture consisted of 2μl of 10X RT buffer, 2μl of dNTP mix (final concentration: 5 mM), 2μl of oligo-dT primer solution (final concentration: 10 μm), 1 μl of RNase inhibitor (final concentration: 10 U / μl), 1μl of Sensiscript reverse transcriptase solution, and aRNA dissolved in sufficient RNase-free water to yield a total volume of 20 μl. Forward and reverse primers for target genes (Table 1) were based on published sequences (42-44) and were obtained from Genemed Synthesis, Inc. (San Francisco, CA, USA). PCR samples consisted of 2μl of cDNA, 10.3μl of RNase / DNase-free water, 0.2μl of each primer, and 12.5μl of iQ SYBR Green Supermix (prod. no. 170-8880; Bio-Rad). PCR reactions were performed in a Bio-Rad iQTM5 iCycler system, with different cyclic parameters for each target. For TrkB, the initial denaturation was 95 °C for 5 min, followed by 40 cycles of 1 min 15 s each (15 s at 54°C followed by 1 min at 60 °C). For BDNF, the initial denaturation was 95 °C for 3 min followed by 50 cycles of 40 s (10 s at 95° C and 30 s at 59° C). The housekeeping gene, GAPDH, was used to normalize mRNA expression in each neurone. In each real-time RT-PCR analysis, no-template and -RT controls were performed. Melt curves generated were analyzed to identify nonspecific products and primer-dimers. The data were analyzed by the $2^-\Delta CT$ method (45). The threshold cycle value (CT) is the number of PCR cycles required for the fluorescence signal to exceed the detection threshold and was set to the log-linear range of the amplification curve. A smaller delta CT value represents higher mRNA expression. 2-ΔCT is determined by subtracting the individual CT value of housekeeping gene (GAPDH) from the corresponding CT value of genes of interest (BDNF and TrkB) and normalized to an internal control.

Plasma measurements

Trunk blood was collected into two centrifuge tubes containing EDTA (Sigma, St Louis, and MO) and centrifuged for 7 min (at 10,000×g) at 4°C. The plasma was removed from each sample, placed into screw top vials and stored at −80°C until it was sent to the University of Iowa RIA Core to be assayed for PRA (plasma rennin activity) and vasopressin (32, 46). A separate sample of whole blood from each rat was collected into a 1.5 ml microcentrifuge tube that did not contain EDTA. Two heparin-containing capillary tubes were filled with blood from this sample for measuring hematocrit. The rest of the sample was centrifuged (5 min; 10,000×g) and a 200 μl sample of plasma was collected for measuring osmolality using a vapor pressure osmometer (Wescor Inc. Logan, UT).

Statistics

Data are presented as group means ± one SEM. The data was analyzed by one-way analysis of variance with Student Newman–Keuls t-test for post hoc analysis of significant main effects (GraphPad PRISM v5.0, GraphPad Software Inc., La Jolla, CA). Significance was set at $P < 0.05$.

RESULTS

Water deprivation increases TrkB and NMDA receptor phosphorylation

Forty-eight hour water deprivation resulted in a marked increase in plasma AVP (Table 1) as well as significant increases in plasma osmolality and hematocrit (Table 2). These data are in agreement with the progressive AVP release into the general circulation from the neurohypophysis during hyperosmolality and hypovolemia related to water deprivation (31, 32). During the rehydration period, animals were given access to water only, not food, for 2 or 4 hours. Rats given 2h access to water drank an average of 28.13 ± 1.06 ml (n=8) and the rats given 4h access to water drank 38.20 ± 2.26 ml (n=5). This difference was statistically significant (P= 0.0008). Access to water for 2 h or 4 h caused hypoosmolality and reduced plasma AVP to control levels without effecting blood volume (Table 3).

LCM was used to harvest RNA from AVP positive neurones from the SON (Figure 1). Subsequent qRT-PCR analysis confirmed the expression of both BDNF (2-ΔCT = 0.00625 ± 0.00132) and TrkB (0.0043 ± 0.00115) in AVP SON neurones. BDNF staining was observed in both vasopressin and non-vasopressin cells in the SON (Figure 2) as previous reported. In euhydrated controls, pTrkBY[515] staining was not evident in cells in the SON (Figure 3, top middle) and there was no co-localization with AVP (Figure 3, bottom right). After water deprivation, pTrkBY[515] staining was observed in cell bodies (Figure 3, bottom middle) and co-localized with AVP in the SON (Figure 3, bottom right).

Brain punches containing the SON were subjected to Western Blot analysis to evaluate the effects of dehydration and rehydration for 2 or 4 hours on TrkB and NMDA receptor subunits NR1 and NR2B. Water deprivation and rehydration were not associated with significant changes in the content of TrkB in the SON (Figure 4A) However, water deprivation increased TrkB phosphorylation (Figure 4A). Access to water for either 2 h or 4 h reduced pTrkBY[515] to control levels (Figure 4A). These results indicate that water deprivation significantly increased the phosphorylation status but not the abundance of TrkB in the SON and that this effect was reversed by water intake.

Similar results were observed for NR1 and NR2B. Water deprivation did not affect NR2B expression (Figure 4B) but was associated with a significant increase in tyrosine phosphorylation of NR2B (pNR2B, Figure 4B) in the SON. Also, 4 h rehydration but not 2 h rehydration decreased pNR2B (Figure 4B) to control levels. While water deprivation and subsequent rehydration did not influence the expression of NR1 (Figure 5), it did increase serine phosphorylation of NR1 (pNR1S[866], Figure 5). This effect was still observed after 2 h of rehydration but was reversed after 4 h of water intake (Figure 5). These data suggest that water deprivation significantly changes the phosphorylation status of TrkB, NR1 and NR2B in the SON and that these effects are reversed by rehydration. The time course of the effects of rehydration suggests that TrkB activation (as indicated by its phosphorylation) may contribute to the phosphorylation of NR1 and NR2B.

Effects of local infusion of TrkB-Fc

Phosphorylation of TrkB receptor can be achieved by means of BDNF binding or transactivation (5, 47). To test whether increased phosphorylation of TrkB associated with water deprivation is mediated by BDNF, a group of animals were instrumented with right SON cannula coupled to mini-osmotic pumps (Alzet model 2004) prefilled with vehicle (0.9% saline) or TrkB-Fc fusion protein (200ng/ul). TrkB-Fc is a fusion protein that consists of an extracellular domain of the TrkB receptor and and Fc domain of IgG. TrkB-Fc binds to BDNF with high affinity and prevents BDNF binding to its receptor. Brain punches that contained the right (cannulated) and left (uncannulated) SON were collected separately from controls and 48hWD rats. In the left SON contralateral to the cannula, TrkB phosphorylation was increased following 48hWD (Figure 6A). The right SON receiving TrkB-Fc showed that the TrkB receptor phosphorylation following 48hWD was significantly attenuated (Figure 6B). These results indicate that TrkB phosphorylation in the SON associated with water deprivation is likely BDNF-mediated.

Similar experiments were conducted to determine if treating the SON with TrkB-Fc would also affect NR1 and NR2B phosphorylation associated with water deprivation. Analysis of the right SON receiving TrkB-Fc showed that the pNR1 receptor phosphorylation following 48hWD was not affected (Figure 6C), while pNR2B was significantly attenuated (Figure 6D). These results suggest that dehydration-induced NR2B phosphorylation in the SON may be BDNF-TrkB mediated.

Possible role of Fyn kinase in BDNF-TrkB regulation of NR2B

Since treating the SON with TrkB-Fc blocked phosphorylation of both TrkB and NR2B, we conducted additional experiments to determine the possible pathway mediating NR2B phosphorylation by TrkB downstream signaling. Therefore, we tested the hypothesis that TrkB receptor-Fyn kinase physical interaction may be affected following dehydration in the SON. Following immunopreciptation of TrkB, membranes were probed with anti-Fyn kinase antibody, stripped and reprobed for NR2B. Immunoblot analysis indicated a physical interaction between Fyn kinase and NR2B and TrkB in the SON of water deprived rats (Figure 7). To check the total amount of TrkB in the assay, 10% of the original lysate were run in parallel for normalization. These results are consistent with the data presented in 1A indicating that TrkB content in the SON is not affected by 48hWD. In a control experiment (data not shown), we obtained similar results for Fyn using 10% total lysate. These data suggest that increased NR2B tyrosine phosphorylation in the SON following dehydration may be due to TrkB-dependent Fyn activation.

DISCUSSION

In order to better understand the possible role of BDNF in the function of SON neurosecretory cells, we examined the effects of 48 h water deprivation on the phosphorylation state of the BDNF receptor TrkB. Our results indicate that water deprivation is associated with a significant increase in TrkB phosphorylation in the SON without changes in TrkB expression. This effect was reversed following 2 h of rehydration with water and blocked by local infusion of TrkB-Fc into the SON. Thus, the present study provides the first evidence that activation of TrkB receptor in the SON following 48 h water deprivation is, at least in part, dependent on BDNF.

Results from our immunohistochemistry and LCM experiments indicate the BDNF and TrkB are expressed in vasopressin MNCs and that water deprivation is associated with increased staining for pTrkBY[515] in vasopressin neurones in the SON. This is consistent with the hypothesis that water deprivation can lead to increased BDNF-TrkB signaling in vasopressin MNCs but our results also indicate that this interaction could occur in oxytocin MNCs as well.

Since the BDNF-TrkB system has been shown to play a significant role in the function of NMDA receptors in other neural systems, we tested the role of water deprivation and local TrkB-Fc infusion on the phosphorylation status of NR1 and NR2B which have previously been shown to be expressed in the SON (27, 48-50). Water deprivation was associated with a significant increase in the serine phosphorylation of NR1 and tyrosine phosphorylation of NR2B without affecting the expression of either subunit. These effects were both reversed by 4 h of rehydration of water. Based on the time course of the rehydration effects on TrkB and NR1/NR2B phosphorylation, we speculated that TrkB activation could be related to the effects of water deprivation on both NR1 and NR2B. However, local TrkB-Fc infusion significantly attenuated only dehydration-induced NR2B phosphorylation. Experiments on cortical and hippocampal homogenates have shown that BDNF exposure increases the amount of Fyn kinase that co-precipitates with TrkB (51). We observed a similar change in the SON following water deprivation. The results of co-immunoprecipitation experiments suggest that TrkB phosphorylation results in phosphorylation of NR2B via Fyn kinase. Although recent evidence supports this pathway (reviewed in (52)), Fyn may also be involved in trafficking TrkB to lipid rafts (51). Therefore, additional experiments will be required to determine the relationship between Fyn kinase and TrkB in the SON. Together these findings support a role for BDNF-TrkB in the phosphorylation of NR2B associated with water deprivation.

BDNF-TrkB signaling in the SON

Phosphorylation of TrkB can result from the binding of either BDNF or neurotrophin 4 (NT-4) or through transactivation (5, 47). In the current study the BDNF scavenger, TrkB-Fc, was infused into the SON to determine TrkB phosphorylation was due to transactivation. Local administration of the TrkB-Fc significantly decreased phosphorylation of TrkB without affecting the contralateral SON. These results suggest a role for BDNF in the phosphorylation of the TrkB in the SON associated with dehydration. The source of BDNF and the possible role of NT4 in the activation of TrkB in the SON remain to be determined.

TrkB-Fc infusion into the SON also attenuate the phosphorylation of NR2B following water deprivation. This suggests that TrkB phosphorylation is necessary for NR2B phosphorylation in the SON related to dehydration. Following activation by BDNF, TrkB dimerizes and activates its internal kinase domain, which then autophosphorylates several specific tyrosine residues, such as the phospholipase C -gamma (PLCγ) site (Y^{816}), the shc site (Y^{515}), and activates Fyn kinases (52, 53). Studies in other systems have demonstrated that Fyn kinase is activated by TrkB (54), it phosphorylates NR2B (55), and contributes to BDNF-induced increases in synaptic transmission (56, 57). These results suggest a similar role for Fyn kinase in the SON although additional studies will be needed to further address this hypothesis.

NMDA receptor internalization is mediated by the tyrosine-based internalization motifs in the C-terminus of NR2 subunits, and NR2B shows stronger internalization and sorting to recycling endosomes. Phosphorylation of this internalization motif in NR2B by Fyn suppresses internalization of NMDA receptors (55). This suggests that phosphorylation of NR2B related to water deprivation could also affect the trafficking of NMDA receptors. Earlier work demonstrated that water deprivation is associated with increased NMDA receptor binding in the SON (58). Additional studies are needed to determine whether or not BDNF-TrkB activation influences NMDA receptor trafficking.

Gene expression studies have shown that NR1 is the most abundant NMDA receptor subunit in the adult SON followed by NR2B, NR2C and NR2D (59), and, it has been reported that in rat SON and PVN NR2B subunit expression is exclusive to MNCs (49). Results from studies using chronic osmotic stimulation show NR1 up-regulation and NR2B down-regulation in homogenates obtained from SON and PVN (27, 60), suggesting that NR2B and NR1-containing NMDA receptors are involved in the osmoregulatory functions of MNCs. No changes in the abundance of NR1 and NR2B were found in the present study or in another recent study that examined changes in NMDA receptor subunits after three days of salt loading (61). These differences could be related to the longer duration of the osmotic stimulation used in the earlier work (7-10 days), the additional physiological changes associated with water deprivation or the antibodies used in the separate studies.

Osmotic stimulation is associated with increases in extracellular glutamate and GABA in the SON (62). Importance of synaptic glutamate receptors in hormone release from the SON was shown by Sladek and colleagues (63) who demonstrated that generalized glutamate receptor blockade with kynurenic acid inhibits vasopressin release during hyperosmotic stimulation. Similarly, Dyball et al. (64) demonstrated that i.c.v. injections of kynurenate decreased the activity of SON neurones subjected to osmotic stimulation. In the SON, NMDA receptors have been shown to affect spike clustering (65) and mediate slow EPSP in putative vasopressin MNCs in response to stimulation of the OVLT (66). Panatier et al. (67) demonstrated that stimulation of the OVLT produces a form of LTP in MNCs that requires NMDA receptor activation. Recent reviews have described several mechanisms that contribute to neuroplasticity of MNCs during physiological challenges such as dehydration and blood loss (68, 69). Phosphorylation of NR2B has been shown to increase time that the

NMDA receptor spends in its active conformation (70). BDNF-TrkB signaling could alter the activity of MNCs in the SON during water deprivation by increasing the postsynaptic effects of NMDA receptors activation and decreasing $GABA_A$ receptor function (7, 14) contributing to plasticity during physiological challenges along with dendritically released peptides and glia associated mechanisms (68, 69). Finally, understanding how osmotically activated TrkB signaling pathways modulate and/or mediate plasticity within the SON and especially for vasopressin neurones may provide new avenues for pharmacological interventions in disease states such as heart or liver failure that are associated with hyponatremia due to inappropriate vasopressin release.

Acknowledgments

References

1. Leibrock J, Lottspeich F, Hohn A, Hofer M, Hengerer B, Masiakowski P, Thoenen H, Barde YA. Molecular cloning and expression of brain-derived neurotrophic factor. Nature. 1989; 341(6238): 149–52. [PubMed: 2779653]

2. Lu B. BDNF and activity-dependent synaptic modulation. Learn Mem. 2003; 10(2):86–98. [PubMed: 12663747]

3. Bramham CR, Messaoudi E. BDNF function in adult synaptic plasticity: the synaptic consolidation hypothesis. Prog Neurobiol. 2005; 76(2):99–125. [PubMed: 16099088]

4. Soule J, Messaoudi E, Bramham CR. Brain-derived neurotrophic factor and control of synaptic consolidation in the adult brain. Biochem Soc Trans. 2006; 34(Pt 4):600–4. [PubMed: 16856871]

5. Numakawa T, Suzuki S, Kumamaru E, Adachi N, Richards M, Kunugi H. BDNF function and intracellular signaling in neurons. Histol Histopathol. 2010; 25(2):237–58. [PubMed: 20017110]

6. Brunig I, Penschuck S, Berninger B, Benson J, Fritschy JM. BDNF reduces miniature inhibitory postsynaptic currents by rapid downregulation of GABA(A) receptor surface expression. Eur J Neurosci. 2001; 13(7):1320–8. [PubMed: 11298792]

7. Hewitt SA, Bains JS. Brain-derived neurotrophic factor silences GABA synapses onto hypothalamic neuroendocrine cells through a postsynaptic dynamin-mediated mechanism. Journal of neurophysiology. 2006; 95(4):2193–8. [PubMed: 16407427]

8. Jovanovic JN, Thomas P, Kittler JT, Smart TG, Moss SJ. Brain-derived neurotrophic factor modulates fast synaptic inhibition by regulating GABA(A) receptor phosphorylation, activity, and cell-surface stability. J Neurosci. 2004; 24(2):522–30. [PubMed: 14724252]

9. Caldeira MV, Melo CV, Pereira DB, Carvalho RF, Carvalho AL, Duarte CB. BDNF regulates the expression and traffic of NMDA receptors in cultured hippocampal neurons. Mol Cell Neurosci. 2007; 35(2):208–19. [PubMed: 17428676]

10. Carvalho AL, Caldeira MV, Santos SD, Duarte CB. Role of the brain-derived neurotrophic factor at glutamatergic synapses. British journal of pharmacology. 2008; 153(Suppl 1):S310–24. [PubMed: 18059328]

11. Klau M, Hartmann M, Erdmann KS, Heumann R, Lessmann V. Reduced number of functional glutamatergic synapses in hippocampal neurons overexpressing full-length TrkB receptors. J Neurosci Res. 2001; 66(3):327–36. [PubMed: 11746350]

12. Marmigere F, Rage F, Tapia-Arancibia L, Arancibia S. Expression of mRNAs encoding BDNF and its receptor in adult rat hypothalamus. Neuroreport. 1998; 9(6):1159–63. [PubMed: 9601686]

13. Yan Q, Radeke MJ, Matheson CR, Talvenheimo J, Welcher AA, Feinstein SC. Immunocytochemical localization of TrkB in the central nervous system of the adult rat. The Journal of comparative neurology. 1997; 378(1):135–57. [PubMed: 9120052]

14. Ohbuchi T, Yokoyama T, Saito T, Hashimoto H, Suzuki H, Otsubo H, Fujihara H, Suzuki H, Ueta Y. Brain-derived neurotrophic factor inhibits spontaneous inhibitory postsynaptic currents in the rat supraoptic nucleus. Brain research. 2009:125834–42.

15. Armstrong WE. Morphological and electrophysiological classification of hypothalamic supraoptic neurons. Progress in Neurobiology. 1995; 47(4-5):291–339. [PubMed: 8966209]

16. Hatton GI. Oxytocin and vasopressin neurones: vive la difference! Journal of Physiology. 1997; 500(Pt 2):284. [PubMed: 9147316]

17. McKinley MJ, Mathai ML, McAllen RM, McClear RC, Miselis RR, Pennington GL, Vivas L, Wade JD, Oldfield BJ. Vasopressin secretion: osmotic and hormonal regulation by the lamina terminalis. Journal of Neuroendocrinology. 2004; 16(4):340–7. [PubMed: 15089972]

18. Bourque CW. Central mechanisms of osmosensation and systemic osmoregulation. Nat Rev Neurosci. 2008; 9(7):519–31. [PubMed: 18509340]

19. Leng G, Brown CH, Bull PM, Brown D, Scullion S, Currie J, Blackburn-Munro RE, Feng J, Onaka T, Verbalis JG, Russell JA, Ludwig M. Responses of magnocellular neurons to osmotic stimulation involves coactivation of excitatory and inhibitory input: an experimental and theoretical analysis. J Neurosci. 2001; 21(17):6967–77. [PubMed: 11517284]

20. Verbalis JG. How does the brain sense osmolality? J Am Soc Nephrol. 2007; 18(12):3056–9. [PubMed: 18003769]

21. Mason WT. Supraoptic neurones of rat hypothalamus are osmosensitive. Nature. 1980; 287(5778): 154–7. [PubMed: 7432448]

22. Aliaga E, Arancibia S, Givalois L, Tapia-Arancibia L. Osmotic stress increases brain-derived neurotrophic factor messenger RNA expression in the hypothalamic supraoptic nucleus with differential regulation of its transcripts. Relation to arginine-vasopressin content. Neuroscience. 2002; 112(4):841–50.

23. Arancibia S, Lecomte A, Silhol M, Aliaga E, Tapia-Arancibia L. In vivo brain-derived neurotrophic factor release and tyrosine kinase B receptor expression in the supraoptic nucleus after osmotic stress stimulus in rats. Neuroscience. 2007; 146(2):864–73. [PubMed: 17346893]

24. Lessmann V. Neurotrophin-dependent modulation of glutamatergic synaptic transmission in the mammalian CNS. General Pharmacology. 1998; 31(5):667–74. [PubMed: 9809461]

25. Crozier RA, Bi C, Han YR, Plummer MR. BDNF modulation of NMDA receptors is activity dependent. Journal of neurophysiology. 2008; 100(6):3264–74. [PubMed: 18842955]

26. Boudaba C, Linn DM, Halmos KC, Tasker JG. Increased tonic activation of presynaptic metabotropic glutamate receptors in the rat supraoptic nucleus following chronic dehydration. J Physiol. 2003; 551(Pt 3):815–23. [PubMed: 12824445]

27. Curras-Collazo MC, Dao J. Osmotic activation of the hypothalamo-neurohypophysial system reversibly downregulates the NMDA receptor subunit, NR2B, in the supraoptic nucleus of the hypothalamus. Brain Res Mol Brain Res. 1999; 70(2):187–96. [PubMed: 10407167]

28. Pak CW, Curras-Collazo MC. Expression and plasticity of glutamate receptors in the supraoptic nucleus of the hypothalamus. Microsc Res Tech. 2002; 56(2):92–100. [PubMed: 11810712]

29. Kuczewski N, Porcher C, Lessmann V, Medina I, Gaiarsa JL. Activity-dependent dendritic release of BDNF and biological consequences. Mol Neurobiol. 2009; 39(1):37–49. [PubMed: 19156544]

30. Nagappan G, Lu B. Activity-dependent modulation of the BDNF receptor TrkB: mechanisms and implications. Trends Neurosci. 2005; 28(9):464–71. [PubMed: 16040136]

31. Dunn FL, Brennan TJ, Nelson AE, Robertson GL. The role of blood osmolality and volume in regulating vasopressin secretion in the rat. J Clin Invest. 1973; 52(12):3212–9. [PubMed: 4750450]

32. Gottlieb HB, Ji LL, Jones H, Penny ML, Fleming T, Cunningham JT. Differential effects of water and saline intake on water deprivation-induced c-Fos staining in the rat. Am J Physiol Regul Integr Comp Physiol. 2006; 290(5):R1251–61. [PubMed: 16306162]

33. Jiang B, Akaneya Y, Ohshima M, Ichisaka S, Hata Y, Tsumoto T. Brain-derived neurotrophic factor induces long-lasting potentiation of synaptic transmission in visual cortex in vivo in young rats, but not in the adult. Eur J Neurosci. 2001; 14(8):1219–28. [PubMed: 11703451]

34. Liang FQ, Allen G, Earnest D. Role of brain-derived neurotrophic factor in the circadian regulation of the suprachiasmatic pacemaker by light. J Neurosci. 2000; 20(8):2978–87. [PubMed: 10751450]

35. Rattiner LM, Davis M, French CT, Ressler KJ. Brain-derived neurotrophic factor and tyrosine kinase receptor B involvement in amygdala-dependent fear conditioning. J Neurosci. 2004; 24(20):4796–806. [PubMed: 15152040]

36. Wang C, Bomberg E, Levine A, Billington C, Kotz CM. Brain-derived neurotrophic factor in the ventromedial nucleus of the hypothalamus reduces energy intake. 2007:R1037–45.

37. Carreno FR, Ji LL, Cunningham JT. Altered central TRPV4 expression and lipid raft association related to inappropriate vasopressin secretion in cirrhotic rats. Am J Physiol Regul Integr Comp Physiol. 2009; 296(2):R454–66. [PubMed: 19091909]

38. Shahar T, House SB, Gainer H. Neural Activity Protects Hypothalamic Magnocellular Neurons against Axotomy-Induced Programmed Cell Death. 2004:6553–62.

39. Paxinos, G.; Watson, C. The rat brain in stereotaxic coordinates. Academic Press, Inc.; San Diego, CA: 1998.

40. Bradford MM. A rapid and sensitive method for the quantitation of microgram quantities of protein utilizing the principle of protein-dye binding. Anal Biochem. 1976:72248–54.

41. Mizuno M, Yamada K, Olariu A, Nawa H, Nabeshima T. Involvement of brain-derived neurotrophic factor in spatial memory formation and maintenance in a radial arm maze test in rats. J Neurosci. 2000; 20(18):7116–21. [PubMed: 10995859]

42. Briski KP, Nedungadi TP, Koshy Cherian A. Effects of Hypoglycaemia on Neurotransmitter and Hormone Receptor Gene Expression in Laser-Dissected Arcuate Neuropeptide Y/Agouti-Related Peptide Neurones. Journal of Neuroendocrinology. 2010; 22(6):599–607. [PubMed: 20298458]

43. Koyama Y, Baba A, Matsuda T. Endothelins stimulate the expression of neurotrophin-3 in rat brain and rat cultured astrocytes. Neuroscience. 2005; 136(2):425–33. [PubMed: 16181740]

44. Zeeni N, Chaumontet C, Moyse E, Fromentin G, Tardivel C, Tome D, Jean A, Darcel N. A positive change in energy balance modulates TrkB expression in the hypothalamus and nodose ganglia of rats. Brain research. 2009:128949–55.

45. Livak KJ, Schmittgen TD. Analysis of Relative Gene Expression Data Using Real-Time Quantitative PCR and the 2-[Delta][Delta]CT Method. Methods. 2001; 25(4):402–8. [PubMed: 11846609]

46. Ji LL, Gottlieb HB, Penny ML, Fleming T, Toney GM, Cunningham JT. Differential effects of water deprivation and rehydration on Fos and FosB/DeltaFosB staining in the rat brainstem. Exp Neurol. 2007; 203(2):445–56. [PubMed: 17027755]

47. Huang EJ, Reichardt LF. Trk receptors: roles in neuronal signal transduction. Annu Rev Biochem. 2003:72609–42.

48. Curras MC, Dao J. Developmental plasticity of NR1 and NR2B subunit expression in the supraoptic nucleus of the rat hypothalamus. Brain Res Dev Brain Res. 1998; 109(1):1–12.

49. Curras-Collazo MC, Chin C, Diaz G, Stivers C, Bozzetti L, Tran LY. Immunolabeling reveals cellular localization of the N-methyl-D-aspartate receptor subunit NR2B in neurosecretory cells but not astrocytes of the rat magnocellular nuclei. The Journal of comparative neurology. 2000; 427(1):93–108. [PubMed: 11042593]

50. Eyigor O, Centers A, Jennes L. Distribution of ionotropic glutamate receptor subunit mRNAs in the rat hypothalamus. The Journal of comparative neurology. 2001; 434(1):101–24. [PubMed: 11329132]

51. Pereira DB, Chao MV. The Tyrosine Kinase Fyn Determines the Localization of TrkB Receptors in Lipid Rafts. The Journal of Neuroscience. 2007; 27(18):4859–69. [PubMed: 17475794]

52. Blum R, Konnerth A. Neurotrophin-mediated rapid signaling in the central nervous system: mechanisms and functions. Physiology (Bethesda). 2005:2070–8.

53. Reichardt LF. Neurotrophin-regulated signalling pathways. Philos Trans R Soc Lond B Biol Sci. 2006; 361(1473):1545–64. [PubMed: 16939974]

54. Narisawa-Saito M, Silva AJ, Yamaguchi T, Hayashi T, Yamamoto T, Nawa H. Growth factor-mediated Fyn signaling regulates alpha-amino-3- hydroxy-5-methyl-4-isoxazolepropionic acid

(AMPA) receptor expression in rodent neocortical neurons. Proc Natl Acad Sci U S A. 1999; 96(5):2461–6. [PubMed: 10051665]

55. Nakazawa T, Komai S, Tezuka T, Hisatsune C, Umemori H, Semba K, Mishina M, Manabe T, Yamamoto T. Characterization of Fyn-mediated tyrosine phosphorylation sites on GluR epsilon 2 (NR2B) subunit of the N-methyl-D-aspartate receptor. J Biol Chem. 2001; 276(1):693–9. [PubMed: 11024032]

56. Wang YT, Salter MW. Regulation of NMDA receptors by tyrosine kinases and phosphatases. Nature. 1994; 369(6477):233–5. [PubMed: 7514272]

57. Alder J, Thakker-Varia S, Crozier RA, Shaheen A, Plummer MR, Black IB. Early presynaptic and late postsynaptic components contribute independently to brain-derived neurotrophic factor-induced synaptic plasticity. J Neurosci. 2005; 25(12):3080–5. [PubMed: 15788764]

58. Meeker RB. Metabotropic and NMDA glutamate receptor interactions with osmotic stimuli in supraoptic neurons. Pharmacol Biochem Behav. 2002; 73(2):475–84. [PubMed: 12117603]

59. Al-Ghoul WM, Meeker RB, Greenwood RS. Differential expression of five N-methyl-D-aspartate receptor subunit mRNAs in vasopressin and oxytocin neuroendocrine cells. Brain Res Mol Brain Res. 1997; 44(2):262–72. [PubMed: 9073168]

60. Decavel C, Curras MC. Increased expression of the N-methyl--aspartate receptor subunit, NR1, in immunohistochemically identified magnocellular hypothalamic neurons during dehydration. Neuroscience. 1997; 78(1):191–202. [PubMed: 9135100]

61. Doherty FC, Sladek CD. NMDA receptor subunit expression in the supraoptic nucleus of adult rats: Dominance of NR2B and NR2D. Brain research. 2011:138889–99.

62. Leng G, Brown CH, Russell JA. Physiological pathways regulating the activity of magnocellular neurosecretory cells. Prog Neurobiol. 1999; 57(6):625–55. [PubMed: 10221785]

63. Sladek CD, Fisher KY, Sidorowicz HE, Mathiasen JR. Osmotic stimulation of vasopressin mRNA content in the supraoptic nucleus requires synaptic activation. Am J Physiol. 1995; 268(4 Pt 2):R1034–9. [PubMed: 7733386]

64. Dyball RE, McKenzie DN, Thomas GP. Osmoresponsiveness of the rat supraoptic nucleus in vivo depends on glutamatergic inputs. Neurobiology (Bp). 1995; 3(3-4):351–62. [PubMed: 8696303]

65. Hu B, Bourque CW. NMDA receptor-mediated rhythmic bursting activity in rat supraoptic nucleus neurones in vitro. J Physiol. 1992:458667–87.

66. Yang CR, Senatorov VV, Renaud LP. Organum vasculosum lamina terminalis-evoked postsynaptic responses in rat supraoptic neurones in vitro. The Journal of Physiology. 1994; 477(Pt 1):59–74. [PubMed: 7915322]

67. Panatier A, Gentles SJ, Bourque CW, Oliet SH. Activity-dependent synaptic plasticity in the supraoptic nucleus of the rat hypothalamus. J Physiol. 2006; 573(Pt 3):711–21. [PubMed: 16613872]

68. Scott V, Brown CH. State-Dependent Plasticity in Vasopressin Neurones: Dehydration-Induced Changes in Activity Patterning. Journal of Neuroendocrinology. 2010; 22(5):343–54. [PubMed: 20088912]

69. Iremonger KJ, Benediktsson AM, Bains JS. Glutamatergic synaptic transmission in neuroendocrine cells: Basic principles and mechanisms of plasticity. Frontiers in Neuroendocrinology. 2010; 31(3):296–306. [PubMed: 20347860]

70. Black IB. Trophic regulation of synaptic plasticity. J Neurobiol. 1999; 41(1):108–18. [PubMed: 10504198]
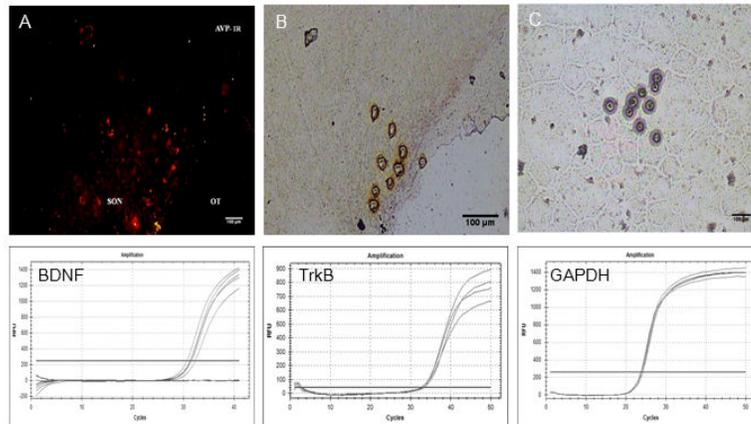
Figure 1.
Top row: Digital images of vasopressin neurones in the SON identified by quick immunostaining (A), dissected by laser capture (B), and captured for later qRT-PCR analysis (C). Bottom row: Relative fluorescence (RFU) amplification curves for BDNF, TrkB, and GAPDH.
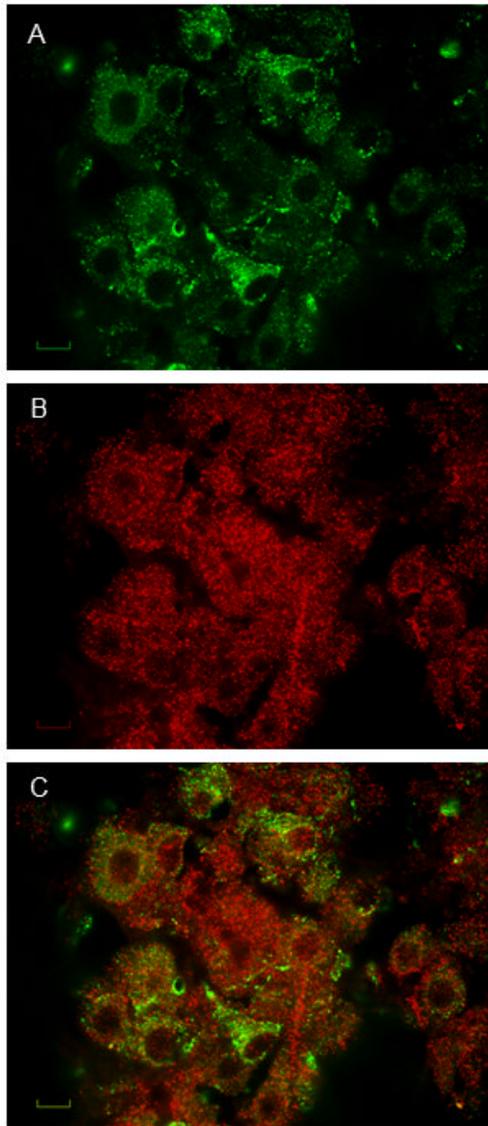
Figure 2.
Pseudocolored digital images depicting immunofluorescence for vasopressin (A, top), BDNF (B, middle), and merged to illustrate vasopressin and BDNF co-localization (C, bottom). Scale bar is 10 μm.
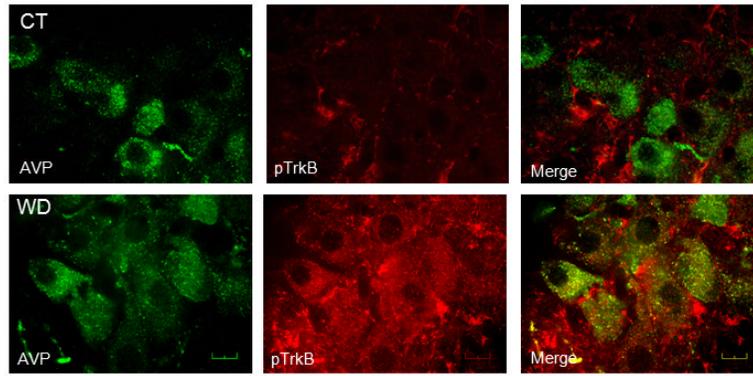
Figure 3.
Digital images demonstrating vasopressin staining (AVP, left column, psuedocollored green), pTrkBY[515] staining (pTrkB, middle column, psuedocolored red), and merged images to illustrate co-localization (Merge, right column) in the SON from a control (CT, top row) and after 48 h water deprivation (WD, bottom row). Scale bar is 20 μm.
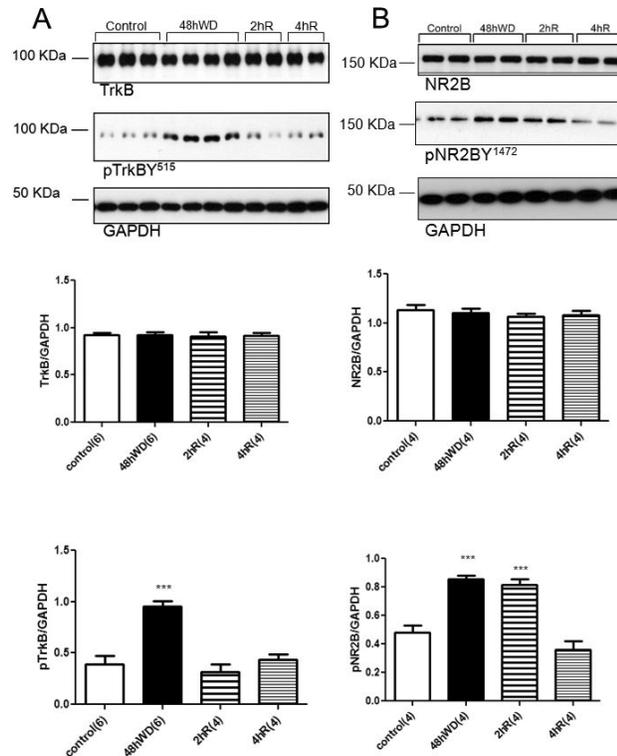
Figure 4.
Tyrosine phosphorylation of TrkB (pTrkBY^{515}) and NR2B (pNR2BY^{1472}) in the SON following water deprivation and rehydration with water. (A) Digital images of representative Western blot analysis for TrkB, pTrkBY^{515}, and GAPDH from brain punches containing the SON from euhydrated control (control), water deprived rats (48hWD) rats, and rats given access to 2h (2hR) or 4h (4hR) water after water deprivation. Graphs represent densitometric analysis of TrkB and pTrkBY^{515} normalized to GAPDH. (B) Digital images of representative Western blots for NR2B, pNR2B and GAPDH from SON samples and graphs of the densitometry for NR2B and pNR2B normalized with GAPDH. *** Statistically significant, P<0.001. Parenthesis indicates number of animals.
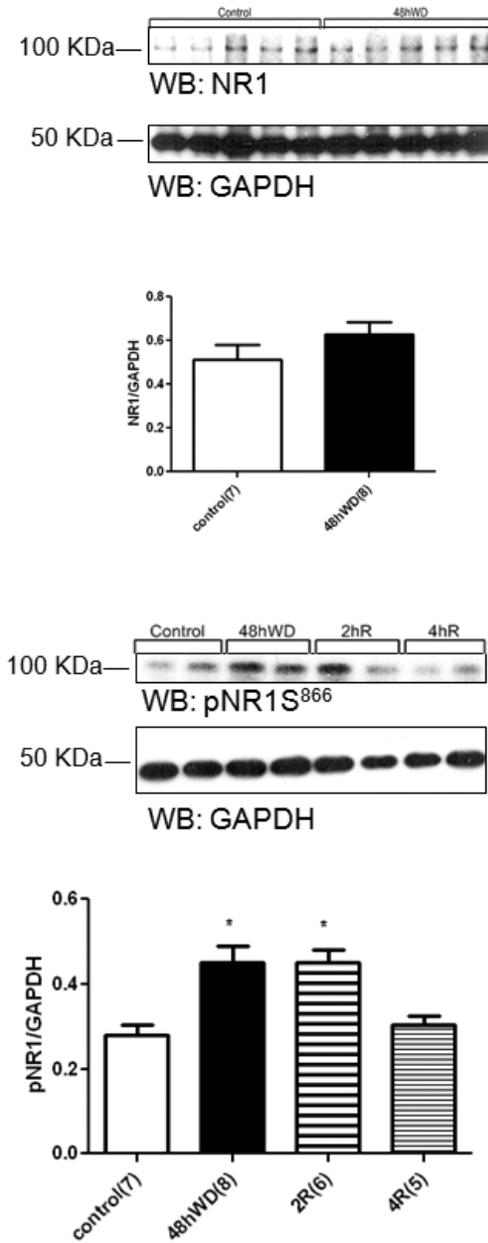
Figure 5.
Serine phosphorylation of NR1 (pNR1S[866]) in the SON from control, water deprivation (48hWD) and rehydration with water for 2 (2R) and 4 (4R) hours. * Statistically significant, P<0.05.
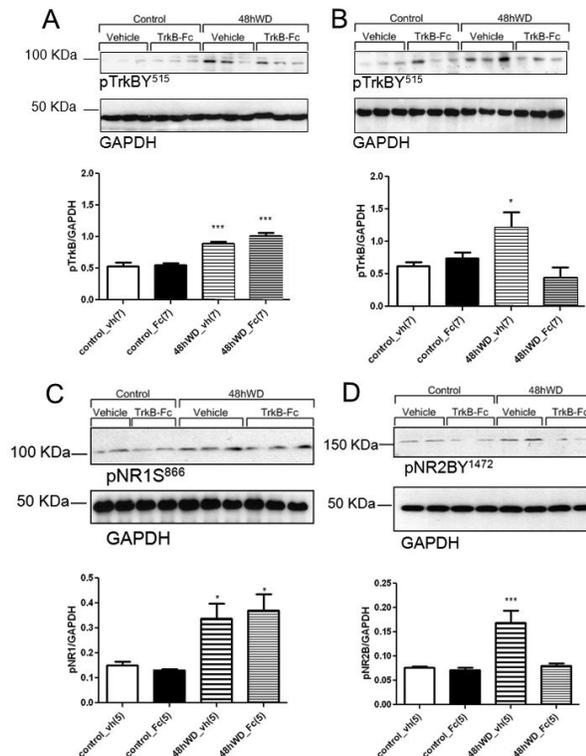
Figure 6.
Effects of chronic, unilateral SON infusion of vehicle (vh) or TrkB-Fc (Fc) on TrkB (A & B), NR1 (C) and NR2B (D) phosphorylation in the SON of euhydrated, controls (controls) water deprived rats (48hWD). Digital images of representative Western blot analysis for pTrkB and GAPDH from the left SON contralateral to the vehicle or TrkB-Fc infusions are in A, while data from the cannulated right SON receiving vehicle or TrkB-Fc are in B. NR1 (C) and NR2B (D) are from the SON ipsilateral to the vehicle or TrkB-Fc infusions. *** Statistically significant, P<0.001, * statistically significant, P<0.05.
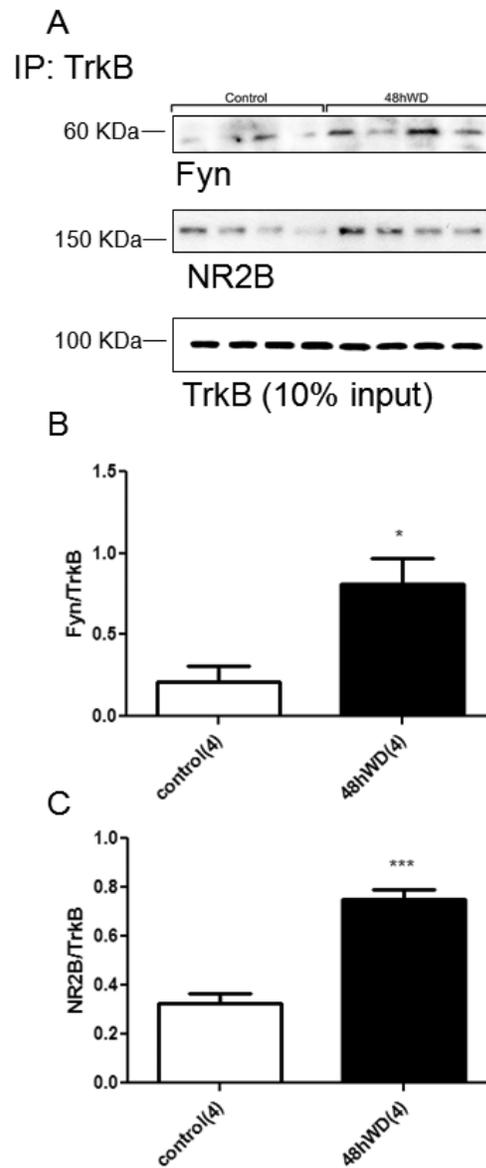
Figure 7.
Co-immunoprecipitation of TrkB and NR2B and Fyn kinase in the SON following 48hWD. (A) Digital images of representative western blot analysis for Fyn kinase, NR2B and TrkB from brain punches containing the SON subjected to co-IP. (B) Graph represents densitometry analysis of physical interaction between Fyn and TrkB in SON subjected to co-IP. Bands of interest were quantified by densitometry using the Scion program. (C) Graph represents densitometric analysis of physical interaction between NR2B and TrkB in SON subjected to co-IP. Bands of interest were quantified by densitometry using the Scion program. *** Statistically significant, P<0.001, * statistically significant, P<0.05. Parenthesis indicates number of samples (each sample represents a pool from two animals of the same treatment group).

Table 1

Forward and reverse primers for qRT-PCR.

TrkB forward primer:	5′-AGCCTTCTCCAGGCATCGT-3′
TrkB reverse primer:	5′-CGGGTCAACGCTGTTAGGTT-3′
BDNF forward primer:	5′-ATGACCATCCTTTTCCTTACTATGGT-3′
BDNF reverse primer:	5′-TCTTCCCCTTTTAATGGTCAGTGTAC-3′
GAPDH forward primer:	5′- ACAGCCGCATCTTCTTGTGC -3′
GAPDH reverse primer:	5′- GCCTCACCCCATTTGATG TT -3

Table 2

Plasma measurements and body weight among groups.

Group	Body weight (g)	Osmolality (mmol/kg)	Hematocrit (%)	AVP (pg/ml)
control	364 ± 7.9 (10)	290 ± 1.2 (10)	43 ± 0.6 (10)	3.6 ± 1.8 (7)
48hWD	304 ± 6.5^a (11)	301 ± 0.6^a (11)	49 ± 0.4^a (11)	58 ± 15 ^{a} (8)
2h Rehydrated	319 ± 13^a (9)	283 ± 1.5^{a,b} (9)	47 ± 0.6^b (9)	13 ± 7.3^b (6)
4h Rehydrated	322 ± 13^a (8)	287 ± 1.3^{a,b}(8)	47 ± 0.58^b (8)	18 ± 10.6^b (4)

Data are mean ± SEM.

^{a}significantly different from control

^{b}significantly different from 48hWD.

Table 3

Plasma measurements and body weight in groups that were instrumented with right SON cannula.

Group	Body weight (g)	Osmolality (mmol/kg)	Hematocrit (%)
Control_vehicle	341 ± 9.7 (7)	293 ± 3.2 (7)	44 ± 1.0 (7)
Control_TrkB-Fc	332 ± 3.8 (7)	291 ± 1.2 (7)	43 ± 1.4 (7)
48hWD_vehicle	307 ± 8.6[a] (7)	307 ± 1.2[a] (7)	48 ± 0.5[a] (5)
48hWD_TrkB-Fc	306 ± 3..8[b] (7)	310 ± 3.2[b] (7)	47 ± 0.8[b] (5)

Data are mean ± SEM.

[a] significantly different from control_vehicle

[b] significantly different from control_TrkB-Fc.